



CHORUS

This is the accepted manuscript made available via CHORUS. The article has been published as:

Maximum Willis Coupling in Acoustic Scatterers

Li Quan, Younes Ra'di, Dimitrios L. Sounas, and Andrea Alù

Phys. Rev. Lett. **120**, 254301 — Published 20 June 2018

DOI: [10.1103/PhysRevLett.120.254301](https://doi.org/10.1103/PhysRevLett.120.254301)

Maximum Willis Coupling in Acoustic Scatterers

Li Quan¹, Younes Ra'di¹, Dimitrios Sounas¹ and Andrea Alù^{1,2,3,4*}

¹*Department of Electrical and Computer Engineering, The University of Texas at Austin,
Austin, Texas 78712, USA*

²*Photonics Initiative, Advanced Science Research Center, City University of New York,
New York, NY 10031, USA*

³*Physics Program, Graduate Center, City University of New York, New York, NY 10026,
USA*

⁴*Department of Electrical Engineering, City College of New York, New York, NY 10031,
USA*

Willis coupling in acoustic materials defines the cross-coupling between strain and velocity, analogous to bianisotropic phenomena in electromagnetics. While these effects have been garnering significant attention in recent years, to date their effects have been considered mostly perturbative. Here, we derive general bounds on the Willis response of acoustic scatterers, show that they can become dominant in suitably designed scatterers, and outline a systematic venue for the realistic implementation of maximally bianisotropic inclusions. We then employ these inclusions to realize acoustic metasurfaces for sound bending with unitary efficiency.

* Corresponding author: aalu@gc.cuny.edu

The emergence of metamaterials and metasurfaces has enabled new opportunities to manipulate electromagnetic waves, providing a rich platform for extreme light-matter interactions [1]-[5]. The fascinating developments in this field have stimulated efforts to apply the same principles to waves of different physical nature, resulting in acoustic and elastic metamaterials. Owing to their unique properties, acoustic metamaterials have enabled unprecedented sound-matter interactions, such as cloaks of inaudibility, acoustic superlenses, acoustic collimators, and nonlinear acoustic phenomena [6]-[14]. In order to realize these artificial materials, various subwavelength resonant inclusions, such as Helmholtz resonators [7],[15], space-coiling structures [16],[17] and membrane-type inclusions [18] have been explored, in order to provide the required enhanced dipole and/or monopole responses.

In electromagnetic metamaterials, an additional knob to tailor the overall metamaterial response has been provided by magneto-electric coupling, or bianisotropy, which enables the coupling of magnetic and electric phenomena at the subwavelength scale. In direct analogy, Willis coupling has been explored in elastodynamics [19]-[22] and acoustics [23]-[25] since the 80s, and it has been recently become of interest in the context of acoustic metamaterials. Willis coupling describes the interaction between acoustic pressure and particle velocity in some acoustic media, and so far it has been treated as a higher-order perturbative phenomenon [22]-[25]. In order to exploit to its full extent bianisotropy in elastodynamics and acoustics, it would be ideal to realize metamaterial inclusions with large, ideally maximum, Willis coupling.

In this Letter, we analyze passive bianisotropic acoustic scatterers, defining a polarizability tensor that relates, in the most general linear scenario, monopole and dipole

moments to the local pressure and velocity. We derive tight bounds on the Willis coupling of small acoustic scatterers imposed by reciprocity and energy conservation, with direct implication on the maximum acoustic bianisotropy achievable in metamaterials formed by such inclusions. These bounds are solely determined by frequency, and are independent of the direct polarizability terms, in contrast to other recent works on bianisotropic metamaterials in electromagnetics [26]. Our bounds show that the pressure-velocity coupling can, in optimized inclusions, be of the same order as the direct polarizability terms. Then, we introduce a general framework to design subwavelength inclusions providing maximum Willis coupling. Finally, we apply these optimal inclusions to design bianisotropic metasurfaces that overcome the inherent efficiency limitations of conventional metasurfaces for arbitrary wavefront manipulation.

Consider a subwavelength particle located in a fluid background and excited by an acoustic wave. Since the particle is small, its scattering can be described by the superposition of acoustic monopole and dipole moments. For non-bianisotropic linear inclusions, the monopole is proportional to the local pressure field, while the dipole is proportional to the local velocity. In the case of Willis coupling, both pressure and velocity fields can excite monopole and dipole moments, and their general relation can be written as

$$\begin{pmatrix} M \\ \mathbf{D} \end{pmatrix} = \boldsymbol{\alpha} \begin{pmatrix} p \\ \mathbf{v} \end{pmatrix} = \begin{pmatrix} \alpha^{pp} & \boldsymbol{\alpha}^{pv} \\ \boldsymbol{\alpha}^{vp} & \boldsymbol{\alpha}^{vv} \end{pmatrix} \begin{pmatrix} p \\ \mathbf{v} \end{pmatrix}. \quad (1)$$

Here $M = \int_V \rho dV$ is the acoustic monopole, $\mathbf{D} = \int_V \rho \mathbf{r} dV$ is the acoustic dipole moment, p is the local pressure, \mathbf{v} is the local velocity, $\boldsymbol{\alpha}$ is the polarizability tensor and ρ is

the density distribution in the particle. The off-diagonal terms $\boldsymbol{\alpha}_{pv}$ and $\boldsymbol{\alpha}_{vp}$ in the polarizability tensor, responsible for Willis coupling, arise when the particle is geometrically asymmetric.

Based on these general relations, we study fundamental constraints imposed by reciprocity and energy conservation over the polarizability tensor of an acoustic inclusion. For simplicity, and without loss of generality, we assume a two-dimensional (2D) scenario, for which the polarizabilities in Eq. (1) can be explicitly written as

$$\begin{pmatrix} M \\ D_x \\ D_y \end{pmatrix} = \begin{pmatrix} \alpha^{pp} & \alpha_x^{pv} & \alpha_y^{pv} \\ \alpha_x^{vp} & \alpha_{xx}^{vv} & \alpha_{xy}^{vv} \\ \alpha_y^{vp} & \alpha_{yx}^{vv} & \alpha_{yy}^{vv} \end{pmatrix} \begin{pmatrix} p \\ v_x \\ v_y \end{pmatrix}. \quad (2)$$

We extend our results to 3D in [27]. Let us first examine the constraints on $\boldsymbol{\alpha}$ imposed by energy conservation. For passive scatterers, the total scattered power must be less or equal than the extinction power $\iint p_s \vec{v}_s^* \cdot d\vec{A} \leq -\iint (p_s \vec{v}_i^* + p_i \vec{v}_s^*) \cdot d\vec{A}$. For a subwavelength scatterer, monopole and dipole moments dominate the scattering, so this relation can be explicitly written as [27]

$$\omega^2 \left(|\sqrt{2}M|^2 + |ik_0 D_x|^2 + |ik_0 D_y|^2 \right) \leq 8 \operatorname{Im} \left[\rho_0 c_0 \vec{v}^* \cdot (ik_0 \vec{D}) - \frac{P^*}{\sqrt{2}} (\sqrt{2}M) \right]. \quad (3)$$

Substituting the monopole and dipole moment expressions from Eq. (2), we get a condition over the polarizabilities of a general acoustic bianisotropic particle [27]

$$\operatorname{Diag} \left[\omega^2 (\boldsymbol{\alpha}^{*T} \boldsymbol{\alpha}') \right] \leq \operatorname{Diag} \left[4i (\boldsymbol{\alpha}'^{T*} - \boldsymbol{\alpha}') \right], \quad (4)$$

where $\boldsymbol{\alpha}'$ is the normalized polarizability tensor defined as

$$\mathbf{\alpha}' = \begin{pmatrix} \alpha_{pp}' & \alpha_x^{pv'} & \alpha_y^{pv'} \\ \alpha_x^{vp'} & \alpha_{xx}^{vv'} & \alpha_{xy}^{vv'} \\ \alpha_y^{vp'} & \alpha_{yx}^{vv'} & \alpha_{yy}^{vv'} \end{pmatrix} = \begin{pmatrix} -2\alpha^{pp} & -\sqrt{2}\alpha_x^{pv}/\rho_0c_0 & -\sqrt{2}\alpha_y^{pv}/\rho_0c_0 \\ ik_0\sqrt{2}\alpha_x^{vp} & ik_0\alpha_{xx}^{vv}/\rho_0c_0 & ik_0\alpha_{xy}^{vv}/\rho_0c_0 \\ ik_0\sqrt{2}\alpha_y^{vp} & ik_0\alpha_{yx}^{vv}/\rho_0c_0 & ik_0\alpha_{yy}^{vv}/\rho_0c_0 \end{pmatrix}. \quad (5)$$

This normalization ensures that all terms in the tensor have the same units. For a reciprocal acoustic particle, the normalized polarizability tensor satisfies $\mathbf{\alpha}' = \mathbf{\alpha}'^{T-}$ [27].

In the non-bianisotropic limit, i.e., in the absence of off-diagonal terms in Eq. (5), the reciprocity condition is always satisfied, and Eq. (4) requires

$$\text{Im}\left(1/\alpha^{pp'}\right) \leq -\omega^2/8 \text{ and } \text{Im}\left(1/\alpha_{xx}^{vv'}\right) = \text{Im}\left(1/\alpha_{yy}^{vv'}\right) \leq -\omega^2/8. \quad (6)$$

These constraints on the imaginary part of the polarizability physically correspond to radiation loss in the particle, and the inequalities become equalities when the particle has no absorption. In the general bianisotropic scenario, we can replace the full polarizability tensor into Eq. (4), resulting in

$$\left\{ \begin{array}{l} \sqrt{|\alpha_x^{vp'}|^2 + |\alpha_y^{vp'}|^2} \leq \sqrt{\frac{-\frac{8}{\omega^2} \text{Im}\left(1/\alpha^{pp'}\right) - 1}{|1/\alpha^{pp'}|^2}} \leq \frac{4}{\omega^2} \\ \sqrt{|\alpha_x^{vp'}|^2 + |\alpha_{xy}^{vv'}|^2} \leq \sqrt{\frac{-\frac{8}{\omega^2} \text{Im}\left(1/\alpha_{xx}^{vv'}\right) - 1}{|1/\alpha_{xx}^{vv'}|^2}} \leq \frac{4}{\omega^2} \\ \sqrt{|\alpha_y^{vp'}|^2 + |\alpha_{xy}^{vv'}|^2} \leq \sqrt{\frac{-\frac{8}{\omega^2} \text{Im}\left(1/\alpha_{yy}^{vv'}\right) - 1}{|1/\alpha_{yy}^{vv'}|^2}} \leq \frac{4}{\omega^2} \end{array} \right. \quad (7)$$

Since $\left| \alpha_x^{vp'} \right|$ and $\left| \alpha_y^{vp'} \right|$ cannot be negative, from the first conditions we derive the same bound as Eq. (6) on the diagonal terms of the polarizability tensor, indicating that these conditions are general, and apply equally well to bianisotropic particles.

The first condition in Eq. (7) imposes also a general bound on the coupling terms. If we assume that the particle is only resonant in the y direction, so that $\left| \alpha_y^{vp'} \right| \gg \left| \alpha_x^{vp'} \right|$, this bound simplifies into $\left| \alpha_y^{vp'} \right| \leq 4\omega^{-2}$. Interestingly, Eq. (7) implies that this limit can be reached only when the particle is at resonance, i.e., when $1/\alpha_{yy}^{vv'} = -i\omega^2/4$ and $1/\alpha^{pp'} = -i\omega^2/4$ are purely imaginary. Substituting these conditions back into the polarizability tensor, we find that optimal Willis scatterers, with maximum bianisotropic coupling, satisfy

$$\begin{pmatrix} \left| \alpha_{pp'} \right| & \left| \alpha_x^{pv'} \right| & \left| \alpha_y^{pv'} \right| \\ \left| \alpha_x^{vp'} \right| & \left| \alpha_{xx}^{vv'} \right| & \left| \alpha_{xy}^{vv'} \right| \\ \left| \alpha_y^{vp'} \right| & \left| \alpha_{yx}^{vv'} \right| & \left| \alpha_{yy}^{vv'} \right| \end{pmatrix} = \frac{4}{\omega^2} \begin{pmatrix} 1 & 0 & 1 \\ 0 & 0 & 0 \\ 1 & 0 & 1 \end{pmatrix}, \quad (8)$$

Interestingly, Eq. (8) confirms that Willis coupling can become of the same order as the diagonal elements of the polarizability tensor, opening new opportunities to enable strong bianisotropy in small acoustic scatterers and metamaterial inclusions. In [27], we extend this analysis and the associated bounds to 3-D inclusions, deriving the analogous bound

$$\left| \alpha_y^{vp'} \right| \leq \frac{6\pi}{c_0^2 k_0^3}.$$

From Eq. (7), we can derive a general bound on the cross-coupling polarizability terms

$$\sqrt{\frac{|\alpha_x^{vp'}|^2 + |\alpha_y^{vp'}|^2}{|\alpha^{pp'}| \sqrt{|\alpha_{xx}^{vv'}|^2 + |\alpha_{yy}^{vv'}|^2}}} \leq \sqrt[4]{\left(-\frac{8}{\omega^2} \text{Im}(1/\alpha^{pp'}) - 1\right) \left[\frac{\left(-\frac{8}{\omega^2} \text{Im}(1/\alpha_{xx}^{vv'}) - 1\right) |\alpha_{xx}^{vv'}|^2 + \left(-\frac{8}{\omega^2} \text{Im}(1/\alpha_{yy}^{vv'}) - 1\right) |\alpha_{yy}^{vv'}|^2 - 2|\alpha_{xy}^{vv'}|^2}{|\alpha_{xx}^{vv'}|^2 + |\alpha_{yy}^{vv'}|^2} \right]} \quad (9)$$

If we suppose again a dominant response along y , so that $\alpha_x^{vp'} \approx 0$, $\alpha_{xx}^{vv'} \approx 0$ and $\alpha_{xy}^{vv'} \approx 0$, this condition simplifies into

$$\frac{|\alpha_x^{vp'}|}{\sqrt{|\alpha^{pp'}| |\alpha_{yy}^{vv'}|}} \leq \sqrt[4]{\left(-\frac{8}{\omega^2} \text{Im}(1/\alpha^{pp'}) - 1\right) \left(-\frac{8}{\omega^2} \text{Im}(1/\alpha_{yy}^{vv'}) - 1\right)}, \quad (10)$$

indicating that, while there is no limit to the normalized Willis response compared to the direct response of the scatterer to pressure and velocity, at resonance, when $|\alpha_x^{vp'}|$ reaches its maximum value $4\omega^{-2}$, we get

$$|\alpha_x^{vp'}| \leq \sqrt{|\alpha^{pp'}| |\alpha_{yy}^{vv'}|}, \quad (11)$$

As an excursus, explorations on the bounds of maximum bianisotropy for small scatterers has been explored in the past years for electromagnetic waves. In [26],[28],[29], a bound consistent with Eq. (11), but for the electromagnetic response, was derived under the assumption of a single coupled electromagnetic resonance in the scatterer. In [30], on the

other hand, it was shown numerically that particles operating far from their resonance frequency or supporting more than one resonance may surpass this bound. Our general theory, if extended to electromagnetics, fully addresses this issue, showing that only Eqs. (7) generally apply, but under the assumption of a single resonant mode the more stringent condition (11) is satisfied.

This general analysis shows that Willis coupling in a small resonant scatterer can be as strong and important as the diagonal terms of the polarizability tensor. In order to exploit the possibilities offered by bianisotropic coupling and create unprecedented sound-matter interactions, we need to design scatterers that approach the fundamental bound derived here. In the following, we show that it is possible to systematically design resonant particles that operate at the bound of maximum Willis coupling coefficient. To shed light into the physical mechanism of bianisotropic coupling in acoustics, consider a 2D cylindrical particle with maze-like channels, shown in Fig. 1a, excited by a standing wave at a pressure node, at which the applied velocity has its maximum. In conventional acoustic subwavelength structures, such a purely velocity field excitation induces only a dipole response. However, if the particle is bianisotropic, an applied background velocity field can generate also a monopole contribution. Since our particle is generally asymmetric, the vibration going in and out of the two channel outlets can have different volume velocities ($2A$ and $2B$ in Fig. 1b). The overall polarization due to the external excitation can be decomposed into dipole and monopole moments, which correspond to the contributions sketched in the center and right column of Fig. 1b.

Let us now consider two special cases. Figure 1c shows the case $A = B$ (i.e., symmetric channel apertures). In this case, only the dipole moment is excited by the applied velocity

field, and therefore the particle has zero Willis coupling. Interestingly, this property is independent of the asymmetry of the internal maze of the particle, and it is guaranteed to first-order approximation as long as the channel width is constant. On the other hand, Fig. 1d shows the case when the apertures are extremely asymmetric, with $B = 0$. For this scenario, the external velocity field produces a dipole response and, in addition, a non-zero monopole response, a direct evidence of Willis coupling.

The insets in Figs. 2a, 2b, and 2c show different geometries providing different levels of bianisotropic coupling. All inclusions have a 5 cm radius and only resonate in the y -direction. The particle in Fig. 2a has a constant channel width, therefore the bianisotropic response is very weak, as seen in the figure. On the other hand, the particle in Fig. 2b is asymmetric, but its bianisotropic response does not reach the bound introduced in the previous section (dashed line in each figure), because the asymmetry is not strong. Finally, the particle in Fig. 2c, provides strong bianisotropic coupling, reaching the theoretical bound at all three resonance frequencies, since one of the apertures is removed. In Fig. 2d, we show the case of a bianisotropic resonant particle with similar asymmetric response in both x - and y - directions. In this case, the general bound in Eq. (7) applies to the sum of the two off-diagonal polarizability elements, where $\alpha_x^{vp'} = \alpha_y^{vp'}$. Details on the polarizability retrieval method used to calculate the results in Fig. 2 are provided in [27], and all simulations have been performed using [31]. The results in Fig. 2 refer to the case of lossless materials. Figure S2 in [27] considers realistic loss in air, showing that, while loss prevents to reach the ideal bound, Willis coupling can stay very strong and comparable with the direct polarizability terms, even in presence of realistic loss.

The systematic design of optimal Willis scatterers introduced here enables translating many of the fascinating opportunities enabled by bianisotropy from electrodynamics to acoustics. In electromagnetic metamaterials, bianisotropic inclusions have been exploited to realize asymmetric absorbing metasurfaces, one-way transparent metasurfaces, and metagratings for perfect control of reflection and refraction [32]-[34]. Exploring analogous effects in acoustics can translate many of these applications to manipulate sound in unprecedented ways. Recently, in electrodynamics it was revealed that conventional gradient metasurfaces designed based on generalized laws of reflection and refraction [35], suffer from fundamental limits on conversion efficiency. A similar limitation has been found in the case of acoustic gradient metasurfaces [36]-[37]. In electrodynamics, bianisotropic metagratings have been proposed to address this issue. These structures are periodic arrays of properly designed bianisotropic inclusions that enable ultimate control over the reflected wave [34], with unitary efficiency even for anomalous reflection towards very large angles.

Here, we translate this idea into acoustics and design an acoustic metagrating based on optimal Willis scatterers capable of rerouting the reflected waves into extreme angles with unitary efficiency. Figure 3 shows the schematic of the designed metagrating, which is composed of a periodic array of the Willis scatterers, similar to Fig. 2(c) with only one outlet, located at a distance from a hard plate. As an example, we design a metagrating that reroutes a normally incident wave to $\theta_{\text{ref}} = \theta_{(-1)} = -72^\circ$ with unitary efficiency. When a periodic array of bianisotropic inclusions over a hard plate is illuminated with a normally incident wave, different Floquet diffraction modes can scatter power away. The periodicity $b = \lambda / \sin \theta_{(1)}$ of the metasurface can be chosen in such a way that the -1 Floquet channel

is aligned with the desired direction of reflection (i.e., $\theta_{(1)} = -\theta_{(-1)} = 72^\circ$). In this scenario, in addition to specular reflection (i.e., 0 channel), -1 and +1 Floquet channels can, in principle, carry power away from the surface, and all other channels are evanescent waves that cannot carry energy away. Therefore, the metasurface can potentially scatter the incident power only through the -1, 0, and +1 diffraction order. Next, we design each scatterer in the array in such a way that its scattering towards the specular direction (i.e., 0 channel) cancels the direct reflection of the incident wave from the hard plate, and such that its scattering in the +1 direction is zero. As a result, all the incident wave is necessarily rerouted to the only available reflection channel, the -1 Floquet order. Fig. 3(b) presents the calculated reflection spectrum for each Floquet channel, calculated with numerical simulations. When the operation frequency is around 2404 Hz, for which the Willis coupling hits a resonance, all incident energy is reflected into the -1 Floquet order, and anomalous reflection with unitary efficiency is achieved.

In conclusion, we have introduced an analytical model for general acoustic scatterers. We studied the restrictions imposed by reciprocity and energy conservation on their polarizabilities, and derived tight theoretical bounds for the acoustic bianisotropic coupling coefficient. It was proven that bianisotropic coupling in acoustics can be of the same order as the diagonal components of the polarizability tensor. This finding paves the way to translate many fascinating opportunities enabled by bianisotropy from electrodynamics to acoustics. Furthermore, we proposed a systematic approach to design realistic scatterers that provide maximum bianisotropic coupling, reaching the theoretical bound introduced in this Letter. As an application of the proposed inclusions, we employed them as building blocks to realize an acoustic metagrating that reroutes a normally incident wave to extreme

directions in reflection with unitary efficiency. This work was supported by the National Science Foundation.

References

- [1] N. Engheta and R. W. Ziolkowski, *Metamaterials: Physics and Engineering Explorations* (IEEE, Piscataway, NJ, 2006).
- [2] N. I. Zheludev and Y. S. Kivshar, From metamaterials to metadevices, *Nature Materials* 11, 917 (2012).
- [3] Y. Zhao, X. -X. Liu, and A. Alù, Recent advances on optical metasurfaces, *J. Opt.* 16, 123001 (2014).
- [4] N. Yu and F. Capasso, Flat optics with designer metasurfaces, *Nat. Mater.* 13, 139 (2014).
- [5] S. B. Glybovski, S. A. Tretyakov, P. A. Belov, Y. S. Kivshar, and C. R. Simovski, Metasurfaces: From microwaves to visible, *Phys. Rep.* 634, 1 (2016).
- [6] J. Li and C. T. Chan, Double-negative acoustic metamaterial, *Phys. Rev. E* 70, 055602(R) (2004).
- [7] N. Fang, D. Xi, J. Xu, M. Ambati, W. Srituravanich, C. Sun, and X. Zhang, Ultrasonic metamaterials with negative modulus, *Nature Mater.* 5, 452-456 (2006).
- [8] M. Ambati, N. Fang, C. Sun, and X. Zhang, Surface resonant states and superlensing in acoustic metamaterials, *Phys. Rev. B* 75, 195447 (2007).
- [9] D. Torrent and J. Sánchez-Dehesa, Acoustic metamaterials for new two-dimensional sonic devices, *New Journal of Physics* 9, 323 (2007).

- [10] S. Zhang, L. Yin, and N. Fang, Focusing ultrasound with an acoustic metamaterial network, *Phys. Rev. Lett.* 102, 194301 (2009).
- [11] S. Zhang, C. Xia, and N. Fang, Broadband acoustic cloak for ultrasound waves, *Phys. Rev. Lett.* **106**, 024301 (2011).
- [12] L. Quan, F. Qian, X. Liu, X. Gong, and P. A. Johnson, Mimicking surface plasmons in acoustics at low frequency, *Phys. Rev. B* 92, 104105 (2015).
- [13] L. Quan, X. Liu, and X. Gong, Quasi-phase-matched backward second-harmonic generation by complementary media in nonlinear metamaterials, *J. Acoust. Soc. Am.* 132, 2852-2856 (2012).
- [14] S. A. Cummer, J. Christensen, and A. Alù, Controlling sound with acoustic metamaterials, *Nature Reviews Materials* 1, 16001 (2016).
- [15] L. Quan, X. Zhong, X. Liu, X. Gong, and P. A. Johnson, Effective impedance boundary optimization and its contribution to dipole radiation and radiation pattern control, *Nature Communications* 5, 3188 (2014).
- [16] Z. Liang and J. Li, Extreme acoustic metamaterial by coiling up space, *Phys. Rev. Lett.* 108, 114301 (2012).
- [17] Y. Xie, B.-I. Popa, L. Zigoneanu, and S. A. Cummer, Measurement of a broadband negative index with space-coiling acoustic metamaterials, *Phys. Rev. Lett.* **110**, 175501 (2013).
- [18] Z. Yang, J. Mei, M. Yang, N. H. Chan, and P. Sheng, Membrane-type acoustic metamaterial with negative dynamic mass, *Phys. Rev. Lett.* 101, 204301 (2008).
- [19] J. R. Willis, Variational principles for dynamic problems for inhomogeneous elastic media, *Wave Motion*, 3, 1-11 (1981).

- [20] G. W. Milton, and J. R. Willis, On modifications of Newton's second law and linear continuum elastodynamic, *Proc. R. Soc. A* 463, 855-880 (2007).
- [21] A. N. Norris, A. L. Shuvalov, A. A. Kutsenko, Analytical formulation of three-dimensional dynamic homogenization for periodic elastic system, *Proc. R. Soc. A* 468, 1629-1651 (2012).
- [22] M. B. Muhlestein, C. F. Sieck, A. Alù, and M. R. Haberman, Reciprocity, passivity and causality in Willis materials, *Proc. R. Soc. A* 472, 20160604 (2016).
- [23] S. Koo, C. Cho, J. Jeong, and N. Park, Acoustic omni meta-atom for decoupled access to all octants of a wave parameter space, *Nat. Commun.* 7, 13012 (2016).
- [24] C. F. Sieck, A. Alù, and M. R. Haberman, Origins of Willis coupling and acoustic bianisotropy in acoustic metamaterials through source-driven homogenization, *Phys. Rev. B* 96, 104303 (2017).
- [25] M. B. Muhlestein, C. F. Sieck, P. S. Wilson, and M. R. Haberman, Experimental evidence of Willis coupling in a one-dimensional effective material element, *Nat. Commun.* 8, 15625 (2017).
- [26] I. Sersic, C. Tuambilangana, T. Kampfrath, and A. F. Koenderink, Magnetolectric point scattering theory for metamaterial scatters, *Phys. Rev. B* **83**, 245102 (2011).
- [27] See Supplementary Material for the detailed derivation of scattered and extinction power, of constraints imposed by energy conservation and reciprocity, polarizability retrieval method, an analogous derivation for 3-D particles, and simulation results using realistic air parameters with dissipation loss taken into account. The Supplementary Material includes Refs. [38-40].

- [28] S. A. Tretyakov, F. Mariotte, C. R. Simovski, T. G. Kharina, and J.-P. Heliot, Analytical Antenna Model for Chiral Scatterers: Comparison with Numerical and Experimental Data, *IEEE Transactions on Antennas and Propagation* 44, 1006 (1996).
- [29] P. A. Belov, S. I. Maslovski, K. R. Simovski, and S. A. Tretyakov, A Condition Imposed on the Electromagnetic Polarizability of a Bianisotropic Lossless Scatterer, *Tech. Phys. Lett.* 29, 718 (2003) (translated from Russian).
- [30] M. Albooyeh, V. S. Asadchy, R. Alaei, S. M. Hashemi, M. Yazdi, M. S. Mirmoosa, C. Rockstuhl, C. R. Simovski, and S. A. Tretyakov, Purely bianisotropic scatterers, *Phys. Rev. B* **94**, 245428 (2016).
- [31] COMSOL Multiphysics 2017, <https://www.comsol.com>.
- [32] Y. Ra'di, V. S. Asadchy, and S. A. Tretyakov, Total absorption of electromagnetic waves in ultimately thin layers, *IEEE Transactions on Antennas and Propagation* 61, 4606 (2013).
- [33] Y. Ra'di, V. S. Asadchy, and S. A. Tretyakov, One-way transparent sheets, *Phys. Rev. B* 89, 075109 (2014).
- [34] Y. Ra'di, D. L. Sounas, and A. Alù, Metagratings: Beyond the limits of graded metasurfaces for wave front control, *Phys. Rev. Lett.* 119, 067404 (2017).
- [35] N. Yu, P. Genevet, M. A. Kats, F. Aieta, J.-P. Tetienne, F. Capasso, and Z. Gaburro, Light propagation with phase discontinuities: Generalized laws of reflection and refraction, *Science* 334, 333 (2011).

- [36] J. Mei and Y. Wu, Controllable transmission and total reflection through an impedance-matched acoustic metasurface, *New Journal of Physics* 16, 123007 (2014).
- [37] Y. Li, X. Jiang, B. Liang, J.-C. Cheng, and L. Zhang, Metascreen-based acoustic passive phased array, *Phys. Rev. Applied* 4, 024003 (2015).
- [38] D. T. Blackstock, *Fundamentals of Physical Acoustics* (Wiley, 2000).
- [39] F. B. Arango and A F. Koenderink, Polarizability tensor retrieval for magnetic and plasmonic antenna design, *New Journal of Physics* 15, 073023 (2013).
- [40] M. S. Mirmoosa, Y. Ra'di, V. S. Asadchy, C. R. Simovski, and S. A. Tretyakov, Polarizabilities of nonreciprocal bianisotropic particles, *Phys. Rev. Applied* 1, 034005 (2014).

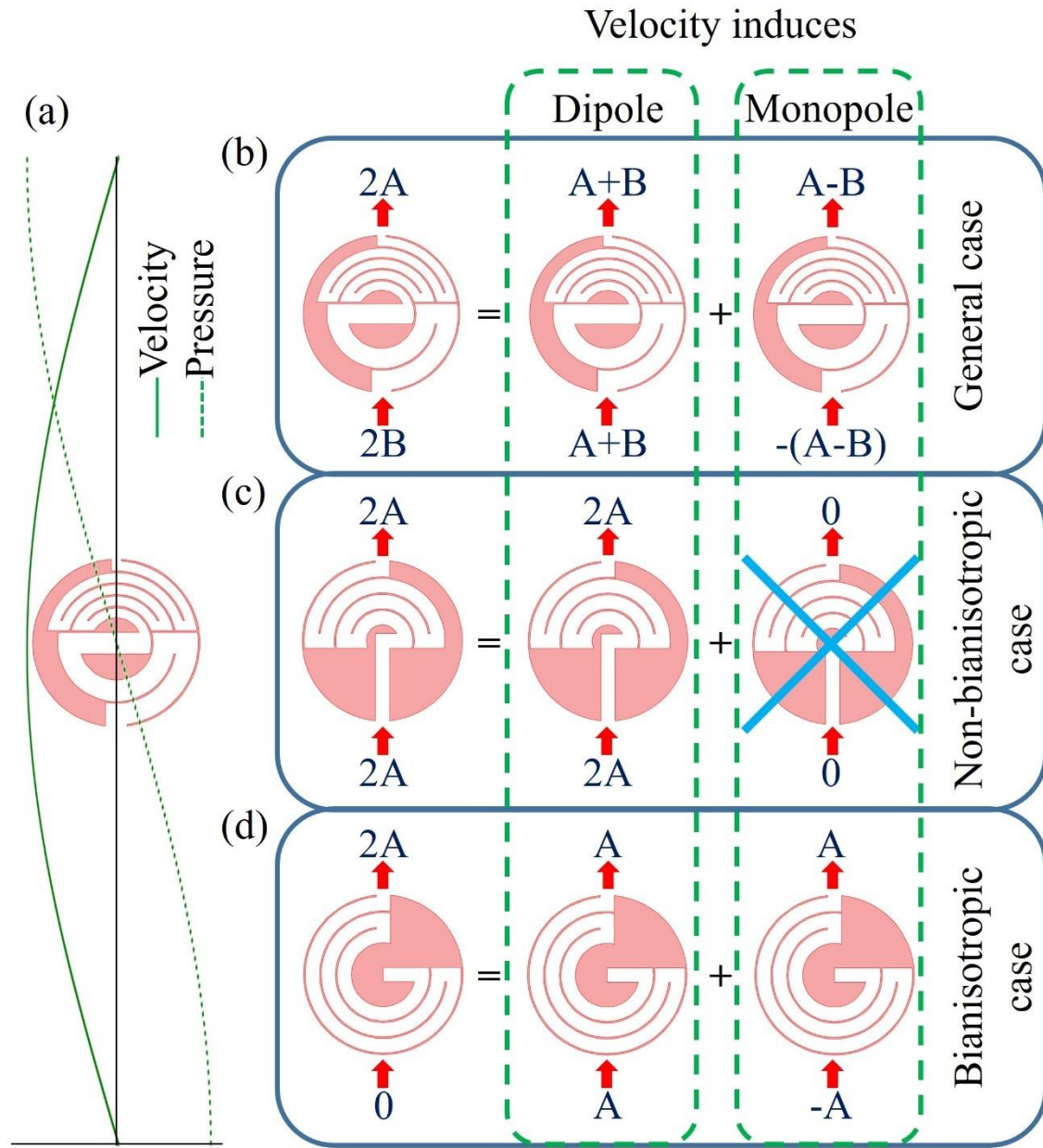


Fig. 1. Physical interpretation of bianisotropic coupling for an acoustic bianisotropic particle. (a) A general bianisotropic particle located in a standing acoustic wave where the applied velocity has its maximum and the pressure is almost zero. (b) A general acoustic particle: Here, $2A$ indicates the total volume velocity coming out from the upper outlet and $2B$ indicates the total volume velocity getting into the lower outlet at a specific instant. (c)

Symmetric acoustic scatterer: Due to the constant width of the channel in the inclusion, the volume velocity for the upper and lower outlets should be identical. In this case, the inclusion is non-bianisotropic because the background velocity field does not excite monopole component. (d) Example of an asymmetric acoustic inclusion: Since the lower outlet is closed, the total volume velocity for lower outlet is zero. By decomposing the zero volume velocity into $-A$ and A , we see that the background volume velocity excites both dipole and monopole components, respectively.

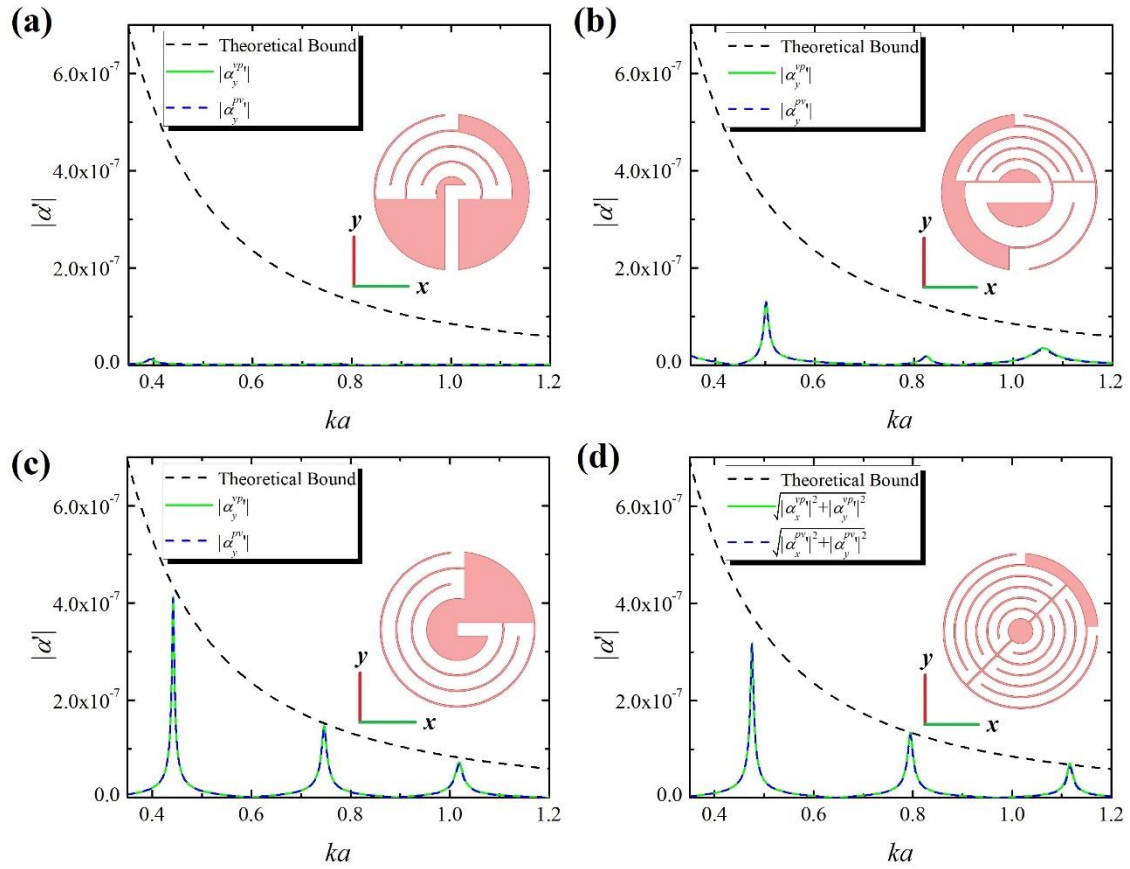


Fig. 2. Comparison of the cross-coupling terms for different bianisotropic inclusions providing different levels of bianisotropic coupling. The radius of all inclusions is 5 cm. (a) Inclusion with constant channel width providing no bianisotropic coupling. (b) Inclusion with different channel width realizing moderate bianisotropic coupling. (c) Inclusion with only one outlet realizing maximum bianisotropy. (d) Inclusion with resonance in two directions.

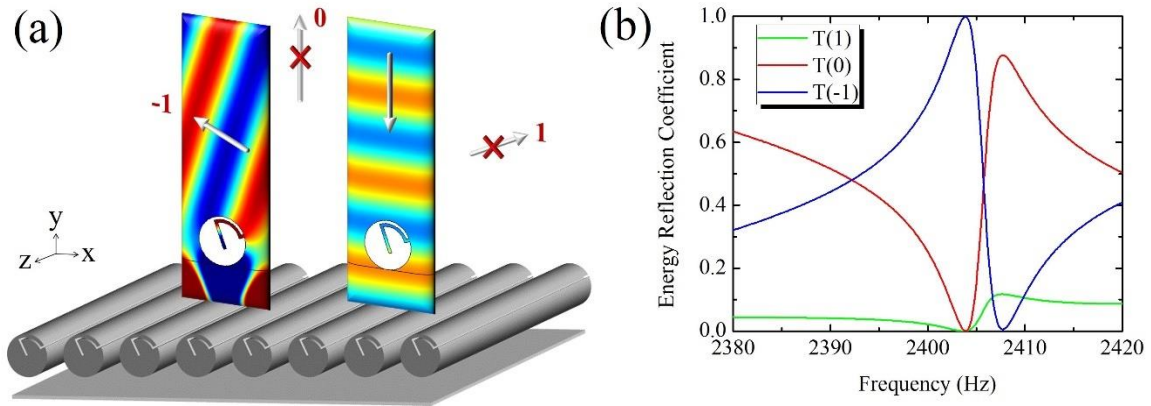


Fig. 3. (a) Schematic of the designed acoustic metagrating, and simulated distribution of incident and reflected pressure fields. Here the period of the grating is chosen to be 15 cm to ensure (-1), (0) and (1) modes are the only modes which can carry out energy, and all other modes are evanescent waves. The bianisotropy inclusion is 4 cm in radius. For a normally incident plane wave, by choosing proper inclusion, unitary reflections can be achieved as shown in the left panel. (b) Normalized reflection spectrum for different Floquet channels. When the operation frequency is near 2404 Hz, all incident energy is reflected into -1 Floquet channel and unitary reflection is achieved.